Analysis of Thermal Dispersion in an Array of Parallel Plates with Fully-Developed Laminar Flow

Jiaying Xu [1], Tian-Jian Lu [2], Howard P. Hodson [1] and Norman A. Fleck [1,*]

[1] *Department of Engineering, University of Cambridge, Trumpington Street, Cambridge, CB2 1PZ, U.K.*
[2] *Department of Applied Mechanics, Xi'an Jiaotong University, Xi'an, Shaanxi Province, 710049, P.R.China*

Abstract

The effect of thermal dispersion on heat transfer across an array of periodically arranged parallel plates is studied in this paper. Three basic heat transfer problems are addressed, each for steady fully-developed laminar fluid flow: (a) transient heat transfer, (b) steady heat transfer with constant heat flux on all plate surfaces, and (c) steady heat transfer with constant wall temperatures. For problems (a) and (b), the effective thermal dispersivity scales with the Peclet number Pe according to $1 + CPe^2$, where the coefficient C is independent of Pe. For problem (c) the coefficient C is a function of Pe. It is demonstrated that both velocity non-uniformity and temperature non-uniformity influence the thermal dispersivity.

Keywords: thermal dispersion, parallel plate array, fully-developed laminar flow, Peclet number

Notation

a	molecular diffusivity, $a = \frac{k}{\rho c}$, $m^2 \cdot s^{-1}$
c	specific heat capacity under constant pressure, $J \cdot kg^{-1} \cdot K^{-1}$
D	half-height of cell containing a fluid and plate, m
H	half-height of unit fluid channel, m
h	heat transfer coefficient along plate surface, $W \cdot m^{-2} \cdot K^{-1}$
k	thermal conductivity, $W \cdot m^{-1} \cdot K^{-1}$
L	length of plate arrays, m
Nu	Nusselt number, $Nu = \frac{h2H}{k_f}$
Pe	Peclet number, $Pe = \frac{u_m 2H}{a_f} = \frac{u_{av} 2D}{a_f}$
Pr	Prandtl number, $Pr = \frac{\nu_f}{a_f} = \frac{Pe}{Re}$
$\dot{Q}$	heat source density in solid plates, W
q	heat flux, $W \cdot m^2$
Re	Reynolds number, $Re = \frac{u_m 2H}{\nu_f} = \frac{u_{av} 2D}{\nu_f}$
T	temperature, K
t	time, s
u	fluid velocity, $m \cdot s^{-1}$
x, y, z	Cartesian coordinates, m

Greek letters

β	ratio of solid to fluid molecular conductivity, $\beta = k_s \big/ k_f$
ε	structure porosity, $\varepsilon = \frac{2H}{2D}$

η	dimensionless space coordinate in y-direction, $\eta = \dfrac{y}{H}$
θ	dimensionless temperature
μ	molecular viscosity, kg·m^{-1}·s^{-1}
ν	kinetic viscosity, m^2·s^{-1}
ξ	dimensionless space coordinate in x-direction, $\xi = \dfrac{x}{L}$
ρ	density, kg·m^{-3}
σ	ratio of two length scales, $\sigma = \dfrac{H}{L}$
Φ	generic variable
ϕ	ratio of solid to fluid heat capacity, $\phi = \left(\rho_s c_s\right) \Big/ \left(\rho_f c_f\right)$
ω_1	dimensionless time coordinate for convection, $\omega_1 = \dfrac{u_m t}{L}$
ω_2	dimensionless time coordinate for diffusion, $\omega_2 = \dfrac{a_f t}{L^2}$

Subscripts

f	fluid
s	solid
eff	effective
av	volume average
m	bulk mean

1. Introduction

The concept of dispersion was first developed for the analysis of mass transfer in porous media [1-3]. Velocity heterogenities within a porous microstructure enhance the mixing of fluid flow, which speeds up the process of mass components spreading from higher concentrations to lower. The so-called dispersion effect is analogous to molecular diffusion. In the analysis of mass dispersion, the focus is shifted from the detailed pore-size (i.e., microscopic) level to the volume-averaged (macroscopic) level. As a result of the averaging process, an effective diffusivity (also called dispersivity) appears naturally in the governing equations.

The process of thermal diffusion is similar to mass diffusion, with concentration distribution replaced by temperature distribution and the corresponding analysis of thermal dispersion developed to study macroscopic heat transfer in porous media. The effective thermal dispersivity is affected by the presence of porosity and flow parameters in addition to the constituent materials; it is the key parameter for dispersion analysis in porous media.

Porous media such as packed beds, cellular foams and lattice materials have complex geometries, making an accurate evaluation of effective dispersivity difficult. To simplify the geometry, idealized geometries are used to represent porous media, for example an array of parallel plates or circular tubes. After volume-averaging, there is no essential difference between the macroscopic response of these idealized models and the more realistic porous structures. The advantage of using idealized models is that analytical solutions at the pore level can be obtained, which can guide the dispersion analysis of porous media having more complicated structures. For example, Taylor [1] studied the transient dispersion of mass along a circular tube, and the results show that the effective dispersivity is a function of flow Peclet number only. The mathematics of thermal dispersion is the same as for mass dispersion, and several attempts have been made to analyse thermal dispersion in simple porous media, as follows. Kurzweg and Jaeger [4] studied the transient response of thermal pulses using a parallel plate array model, and obtained exact correlation of the effective thermal

dispersion conductivity. Yuan et al. [5] analytically studied thermal dispersion using thick-walled tubes, for both transient and steady heat transfer, and obtained asymptotic solutions. They found that the non-dimensional dispersive term has the form of $1 + CPe^2$, where Pe is the Peclet number and the proportionality coefficient C depends upon the aspect ratio of tube cross-section, the fluid and thermal properties of the tube and upon the temperature field. Batycky et al. [6] used the Taylor expansion technique to study the dispersion in a circular cylinder and confirmed the Pe^2 dependence.

All of the above studies on thermal dispersion are based on transient analysis where the temperature of the incoming fluid undergoes a step-wise change and the subsequent temperature field is determined as a function of space and time (while the underlying fluid flow is steady and generally considered laminar). The so-obtained thermal dispersivity is then applied to steady-state heat transfer in porous media [7-11]. The validity of this approach is assessed in the current paper. For simplicity, a parallel plate array serves as the prototypical porous medium, with underlying fully-developed laminar fluid flow. Both transient and steady heat transfers are analysed. In the steady state analysis, the effects of applying different thermal boundary conditions are examined. In addition, the effect of porosity of the idealized porous medium upon thermal dispersivity is quantified.

2. Problem description

Consider steady-state laminar flow through an array of equi-spaced parallel plates, as shown in Fig. 1 along with the coordinate system. We shall refer to the plate material as the solid phase and the moving liquid between the stationary plates as the fluid phase, and use superscripts and subscripts s and f to denote the solid and fluid, respectively. We assume that the plates are sufficiently large in both the stream-wise x-direction and the span-wise z-direction, and also assume that the number of plates in the cross-flow y-direction is large. Under these conditions, the problem can be

considered as two-dimensional in the (x, y) plane; also, the flow is taken to be fully developed, with entry and exit effects ignored. Periodicity in the y-direction allows for volume averaging, with the integration performed over a unit channel only, $-D \le y \le D$, where $2D$ is the height of the unit cell. The problem thereby reduces to pseudo-one-dimensional after volume averaging.

Consider fully-developed laminar flow in a channel of width $2H$ with bulk mean fluid velocity u_m, see Fig.1. The stream-wise velocity u_f of the fluid within a representative channel varies parabolically with distance y from the mid-plane of the channel according to:

$$u_f = \frac{3}{2} u_m \left(1 - \frac{y^2}{H^2}\right), \text{ for } -H \le y \le H . \tag{1}$$

The cross-flow velocity of the fluid is zero everywhere, as well as the span-wise velocity. The overall average velocity for the whole array is $u_{av} = \frac{H}{D} u_m$ since the solid plates are taken to be stationary.

Assume that no heat sources exist in the fluid phase and that heat sources of uniform density $\dot{Q}$ exist within the solid plates. Then, the temperature T_s in the solid phase and the temperature T_f in the fluid phase satisfy

$$\frac{\partial T_s}{\partial t} - \frac{\dot{Q}}{\rho_s c_s} = a_s \left(\frac{\partial^2 T_s}{\partial x^2} + \frac{\partial^2 T_s}{\partial y^2}\right), \qquad \text{for } H \le |y| \le D, \tag{2}$$

$$\frac{\partial T_f}{\partial t} + u_f \frac{\partial T_f}{\partial x} = a_f \left(\frac{\partial^2 T_f}{\partial x^2} + \frac{\partial^2 T_f}{\partial y^2}\right), \qquad \text{for } |y| \le H, \tag{3}$$

where t is time, $a = \frac{k}{\rho c}$ is the molecular diffusivity, and ρ, c and k are material density, specific heat under constant pressure and molecular conductivity, respectively.

It is assumed that there is no jump in temperature and in heat flux at the plate surfaces:

$$T_s\Big|_{y=\pm H} = T_f\Big|_{y=\pm H}, \text{ and } -k_s \left.\frac{\partial T_s}{\partial y}\right|_{y=\pm H} = -k_f \left.\frac{\partial T_f}{\partial y}\right|_{y=\pm H}. \tag{4}$$

3. Volume averaging and the effective thermal dispersion

A general expression for the effective thermal dispersion is now determined in terms of volume-averaged quantities. In subsequent sections, particular explicit expressions are obtained for restricted choices of boundary condition and initial condition.

3.1. Volume averaging procedure

Introduce the operator $\langle\ \rangle$, absent a superscript s or f, to denote volume-averaging over both phases, as follows. We consider the following y-direction averaging over one channel $-D < y < D$:

$$\left\langle \boldsymbol{\Phi} \right\rangle = \frac{1}{2D}\int_{-D}^{D} \boldsymbol{\Phi} dy = \frac{1}{D}\int_{0}^{D} \boldsymbol{\Phi} dy, \tag{5}$$

where $\boldsymbol{\Phi}$ is a general variable, such as velocity u or temperature T. For example, the average velocity of the fluid and solid is $u_{av} = \left\langle u \right\rangle$. The averaging procedure splits a variable into two parts, the averaged value and the perturbed value $\boldsymbol{\Phi} = \left\langle \boldsymbol{\Phi} \right\rangle + \boldsymbol{\Phi}'$.

Averaging is also performed over each phase, and this is known as *intrinsic* volume averaging. Denote $\left\langle \boldsymbol{\Phi} \right\rangle^s$ as the volume-average over the solid phase, and $\left\langle \boldsymbol{\Phi} \right\rangle^f$ as the volume-average over the fluid phase, such that

$$\left\langle \boldsymbol{\Phi} \right\rangle^s = \frac{1}{2\left(D-H\right)}\left(\int_{H}^{D} \boldsymbol{\Phi} dy + \int_{-D}^{-H} \boldsymbol{\Phi} dy\right) = \frac{1}{D-H}\int_{H}^{D} \boldsymbol{\Phi} dy, \tag{6}$$

and

$$\left\langle \boldsymbol{\Phi} \right\rangle^f = \frac{1}{2H}\int_{-H}^{H} \boldsymbol{\Phi} dy = \frac{1}{H}\int_{0}^{H} \boldsymbol{\Phi} dy \tag{7}$$

Here, we have already taken the advantage of the symmetry characteristics of flow over the mid-plane $y = 0$.

Write Φ_f as the value of Φ within the fluid phase and assume compact support such that $\Phi_f = 0$ in the solid phase. Likewise, write Φ_s as the value of Φ within the solid phase and assume that $\Phi_s = 0$ in the fluid phase. Then, the intrinsic and overall volume-averaged variables are related by:

$$\left\langle \Phi_f \right\rangle^f = \frac{1}{\varepsilon}\left\langle \Phi_f \right\rangle, \tag{8}$$

$$\left\langle \Phi_s \right\rangle^s = \frac{1}{1-\varepsilon}\left\langle \Phi_s \right\rangle, \tag{9}$$

where $\varepsilon = H \,/\, D$ is the structural porosity, defined as the ratio of void volume to the overall volume. Note that $\left\langle \Phi_s \right\rangle^f = 0$ and $\left\langle \Phi_f \right\rangle^s = 0$. Additional features of volume-averaging are given in Appendix A.

3.2. Effective thermal dispersion

In some porous models, there exists local thermal equilibrium where the net energy transfer between fluid phase and solid phase is zero. In these cases, we have $\left\langle T \right\rangle^f = \left\langle T \right\rangle^s = \left\langle T \right\rangle$; Consequently the two separate energy conservation equations for each phase can be merged into one, yielding to the so-called one-equation models [12, 13]. In other cases of local thermal non-equilibrium, $\left\langle T \right\rangle^f \neq \left\langle T \right\rangle^s$. Hence there exists non-zero net energy transfer from one phase to another. A two-equation model has to be used for these cases [11, 14, 15].

We can follow the theoretical work of Whitaker and his co-workers ([11, 12, 14, 16]) and Moyne *et al* [12], in order to evaluate the hydraulic dispersion effect upon heat

transfer in parallel plate arrays. For example, the energy equation after volume averaging can be written as below:

$$\left\langle \rho c \right\rangle \frac{\partial \left\langle T \right\rangle}{\partial t} - \left(1-\varepsilon\right)\dot{Q} + \rho_f c_f \frac{\partial \left(\left\langle u \right\rangle \left\langle T \right\rangle + \varepsilon \left\langle u_f{}' T_f{}' \right\rangle \right)}{\partial x} = \left\langle k \right\rangle \frac{\partial^2 \left\langle T \right\rangle}{\partial x^2}, \tag{10}$$

where $\left\langle \rho c \right\rangle = \left[\left(1-\varepsilon\right)\rho_s c_s + \varepsilon \rho_f c_f \right]$ and $\left\langle k \right\rangle = \left[\left(1-\varepsilon\right)k_s + \varepsilon k_f \right]$ are the volume-averaged heat capacity and molecular conductivity, respectively. Equation (10) can be rewritten as:

$$\frac{\partial \left\langle T \right\rangle}{\partial t} + u_{av} \frac{\partial \left\langle T \right\rangle}{\partial x} = \left\langle a \right\rangle \frac{\partial^2 \left\langle T \right\rangle}{\partial x^2} - \frac{\varepsilon \rho_f c_f}{\left\langle \rho c \right\rangle} \frac{\partial \left\langle u_f{}' T_f{}' \right\rangle}{\partial x} + \frac{\dot{Q}\left(D-H\right)}{\left(D-H\right)\rho_s c_s + H \rho_f c_f}, \tag{11}$$

where $\left\langle a \right\rangle = \dfrac{\left\langle k \right\rangle}{\left\langle \rho c \right\rangle}$ is the volume-averaged molecular diffusivity.

Eq. (11) can be further rewritten as

$$\frac{\partial \left\langle T \right\rangle}{\partial t} + u_{av} \frac{\partial \left\langle T \right\rangle}{\partial x} = a_{eff} \frac{\partial^2 \left\langle T \right\rangle}{\partial x^2} + \frac{\dot{Q}\left(D-H\right)}{\left(D-H\right)\rho_s c_s + H \rho_f c_f}, \tag{12}$$

where $a_{eff} = \dfrac{k_{eff}}{\left(\rho c\right)_{eff}}$ is the effective diffusivity and can be evaluated via the following equation:

$$a_{eff} \frac{\partial \left\langle T \right\rangle}{\partial x} = \left\langle a \right\rangle \frac{\partial \left\langle T \right\rangle}{\partial x} - \frac{\varepsilon \rho_f c_f}{\left\langle \rho c \right\rangle} \left\langle u_f{}' T_f{}' \right\rangle, \tag{13}$$

or, in non-dimensional form,

$$\frac{a_{eff}}{\left\langle a \right\rangle} = 1 - \frac{\varepsilon \rho_f c_f}{\left\langle k \right\rangle} \frac{\left\langle u_f{}' T_f{}' \right\rangle}{\partial \left\langle T \right\rangle / \partial x} = 1 + \frac{\varepsilon \rho_f c_f}{\left\langle k \right\rangle} \frac{\left\langle u \right\rangle \left\langle T \right\rangle - \left\langle u_f T_f \right\rangle}{\partial \left\langle T \right\rangle / \partial x}. \tag{14}$$

The left hand side of Eq. (14) is the relative effective thermal dispersivity. The number unity on the right hand side of Eq. (14) addresses the (relative) molecular diffusivity while the second term measures the pure dispersion effect. Thus, the above expression reveals that the effective diffusivity comprises both the molecular diffusivity and the

dispersion effect.

Equation (12) describes a macroscopically one-dimensional problem. Additionally, the velocities and pressure gradient remain constant along the stream-wise x-direction within the fully developed region. As far as heat transfer is concerned, the type of variable that remains constant depends on the underlying thermal condition: for constant heat flux condition, it is the temperature gradient and for constant wall temperature condition, the dimensionless excess temperature (defined as the ratio of the difference between a local temperature and the wall temperature to the difference between the bulk mean temperature and the same wall temperature, all at the same x-position). The original two-dimensional problem has been transformed to a new one-dimensional one, with all variables now only dependent upon the x coordinate. Since this one-dimensionality is only valid from a macroscopic point of view (that is, after averaging), we call the original problem a pseudo-one-dimensional problem.

Focusing now on the macroscopically one-dimensional problem, we analyze the energy balance in a small volume δx in the flow direction over a small time period δt, as illustrated in Fig. 2. The net energy increase due to conduction and convection is $2D \cdot k_{eff} \cdot \dfrac{\partial^2 \langle T \rangle}{\partial x^2} \cdot \delta x \cdot \delta t$ and $2D \cdot (\rho c)_{eff} \cdot u_{av} \dfrac{\partial \langle T \rangle}{\partial x} \cdot \delta x \cdot \delta t$, respectively; that due to internal heat source in the solid plates is $2(D-H) \cdot \dot{Q} \cdot \delta x \cdot \delta t$; the total energy increase is $2D \cdot (\rho c)_{eff} \cdot \dfrac{\partial \langle T \rangle}{\partial t} \cdot \delta x \cdot \delta t$, where $\langle T \rangle$ denotes the temperature from the macroscopic point of view, and k_{eff}, $(\rho c)_{eff}$ are separately the effective thermal conductivity and heat capacity, $k_{eff} = (\rho c)_{eff} \cdot a_{eff}$. Based on the conservation of energy we recover Eq. (12). The last term in Eq. (12), $\dfrac{\dot{Q}(D-H)}{(D-H)\rho_s c_s + H \rho_f c_f}$, can be interpreted as the internal source converted from the heat density of plates. It is noteworthy that the volume-averaged temperature $\langle T \rangle$ is the macroscopic temperature.

In order to understand the physical meaning of thermal dispersion, we take a close examination of the second term on the right hand side of Eq. (14). The pure dispersivity is inversely proportional to the heat flux density along the flow direction, $\left\langle k \right\rangle \frac{\partial \left\langle T \right\rangle}{\partial x}$, and proportional to the difference between the uniformly distributed heat flux and the volume-averaged heat flux. As illustrated in Fig. 3, the uniformly distributed heat flux is contained within the vertical bar (shadowed region), whilst the volume-averaged heat flux is contained within the parabolic-shaped shadow area. The dispersion concept quantifies the microscopic non-uniformity of the heat flux distribution. There is no dispersion in a porous medium if either the velocity or temperature is uniformly distributed at the microscopic (pore) level. The non-uniformity of velocity distribution within each fluid channel is a consequence of the porous structure; whilst the non-uniformity of temperature distribution can be attributed to both the velocity non-uniformity and the thermal boundary conditions.

In the following section, the role of effective thermal dispersivity and the physical mechanisms of thermal dispersion are explored further by developing analytical solutions to several particular cases of the parallel plate model.

4. Transient heat transfer across an array of parallel plates

If a thermal disturbance occurs within the porous medium model (assuming no heat source within the solid plates), for example a thermal pulse is introduced at the entrance of the parallel plate array, then this disturbance will spread through the system. Within a sufficiently short initial period, the thermal transient traveling across the system is similar to the phenomenon of thermal penetration across a semi-infinite solid plate. Thermal penetration into the system becomes faster due to velocity non-uniformity, in comparison with a plug flow which has a uniform velocity distribution. Zanotti and Carbonell [17-19] revealed that, after a sufficiently long time period, the thermal pulse will travel at the same speed in both phases.

In order to obtain analytical results, the first step is to non-dimensionalize the governing equations. The spatial coordinates are non-dimensionalized as:

$$\xi = \frac{x}{L};\ \eta = \frac{y}{H}, \tag{15}$$

where the plate length L is a length scale at the structural level, and is usually much larger than the length scale at the pore level, i.e. $L \gg D \sim H$. The time coordinate is converted to two independent timescales:

$$\omega_1 = \frac{u_m t}{L};\ \omega_2 = \frac{a_f t}{L^2}, \tag{16}$$

where ω_1 is the non-dimensional timescale for convection along the flow direction and ω_2 is the non-dimensional timescale for molecular diffusion. Application of the chain rule of differentiation with respect to time results in:

$$\frac{\partial \Phi}{\partial t} = \frac{\partial \Phi}{\partial \omega_1}\frac{d\omega_1}{dt} + \frac{\partial \Phi}{\partial \omega_2}\frac{d\omega_2}{dt} = \frac{u_m}{L}\frac{\partial \Phi}{\partial \omega_1} + \frac{a_f}{L^2}\frac{\partial \Phi}{\partial \omega_2}.$$

The reasons to use two different length scales and two different time scales are:

1) Heat transfer mechanisms in the x- and y-directions are different: heat transfer along the x-direction is by both convection and conduction, the former being dominant; in the y-direction, only conduction occurs.
2) The traveling speeds of heat flow are different for convection and diffusion. Generally the former is much faster than the latter.
3) Consequently, different physical phenomena will be separated in the governing equations by using different length and time scales.

We introduce some useful dimensionless parameters for later convenience: Reynolds number, $Re = \frac{u_{av} 2D}{\nu_f} = \frac{u_m 2H}{\nu_f}$; Prandtl number, $Pr = \frac{\nu_f}{a_f} = \frac{\mu_f c_f}{k_f}$; Peclet number, $Pe = \frac{u_{av} 2D}{a_f} = \frac{u_m 2H}{a_f} = RePr$; Nusselt number, $Nu = \frac{2Hh}{k_f}$, where ν_f and μ_f are

the kinematical and molecular fluid viscosity, with $\nu_f = \frac{\mu_f}{\rho_f}$; h is the averaged heat transfer coefficient along the plate surface.

The governing equations Eqs. (2) and (3), with the source term removed in Eq. (2), are thereby non-dimensionalized into the form:

$$\frac{Pe}{2}\sigma\frac{\partial T_f}{\partial \omega_1} + \sigma^2\frac{\partial T_f}{\partial \omega_2} + \frac{3Pe}{4}\sigma\left(1-\eta^2\right)\frac{\partial T_f}{\partial \xi} = \sigma^2\frac{\partial^2 T_f}{\partial \xi^2} + \frac{\partial^2 T_f}{\partial \eta^2},\ \text{for } 0 \le \eta \le 1, \quad (17)$$

$$\frac{Pe}{2\phi}\sigma\frac{\partial T_s}{\partial \omega_1} + \frac{\sigma^2}{\phi}\frac{\partial T_s}{\partial \omega_2} = \sigma^2\frac{\partial^2 T_s}{\partial \xi^2} + \frac{\partial^2 T_s}{\partial \eta^2},\ \text{for } 1 \le \eta \le \frac{1}{\varepsilon}, \quad (18)$$

where $\sigma = \frac{H}{L}$ and $\phi = \frac{a_s}{a_f}$. Similarly, the boundary conditions become:

$$T_s\big|_{\eta=1} = T_f\big|_{\eta=1},\ \left.\frac{\partial T_f}{\partial \eta}\right|_{\eta=1} = \beta\left.\frac{\partial T_s}{\partial \eta}\right|_{\eta=1} \quad (19)$$

for interfacial boundaries, where $\beta = \frac{k_s}{k_f}$, and

$$\left.\frac{\partial T_f}{\partial \eta}\right|_{\eta=0} = 0,\ \left.\frac{\partial T_s}{\partial \eta}\right|_{\eta=\frac{1}{\varepsilon}} = 0, \quad (20)$$

for symmetric boundaries.

We consider the asymptotic expansions of temperatures T_f and T_s in powers of the free parameter σ,

$$T_f = T_{f0} + T_{f1}\sigma + T_{f2}\sigma^2 + T_{f3}\sigma^3 + \cdots \quad (21)$$

$$T_s = T_{s0} + T_{s1}\sigma + T_{s2}\sigma^2 + T_{s3}\sigma^3 + \cdots, \quad (22)$$

where T_f, T_s, T_{f0}, T_{s0}, T_{f1}, T_{s1}, … are each functions of ξ, η, ω_1 and ω_2. The expansions rapidly converge as the value of σ is small.

Upon substituting Eqs. (21) and (22) into Eqs. (17) and (18), we collect terms in like powers of σ, and this leads to a hierarchy of linear differential equation sets. Since σ is a free parameter, the boundary conditions must be satisfied at each power of σ.

At level σ^0:

$$\begin{cases} \dfrac{\partial^2 T_{f0}}{\partial \eta^2} = 0, \quad \text{for } 0 \le \eta \le 1, \\ \dfrac{\partial^2 T_{s0}}{\partial \eta^2} = 0, \quad \text{for } 1 \le \eta \le \dfrac{1}{\varepsilon}, \\ T_{s0}\Big|_{\eta=1} = T_{f0}\Big|_{\eta=1}, \quad \dfrac{\partial T_{f0}}{\partial \eta}\Big|_{\eta=1} = \beta \dfrac{\partial T_{s0}}{\partial \eta}\Big|_{\eta=1}, \\ \dfrac{\partial T_{f0}}{\partial \eta}\Big|_{\eta=0} = 0, \quad \dfrac{\partial T_{s0}}{\partial \eta}\Big|_{\eta=\frac{1}{\varepsilon}} = 0. \end{cases}$$

At level σ^1:

$$\begin{cases} \dfrac{\partial^2 T_{f1}}{\partial \eta^2} - \dfrac{Pe}{2}\dfrac{\partial T_{f0}}{\partial \omega_1} - \dfrac{3Pe}{4}\left(1-\eta^2\right)\dfrac{\partial T_{f0}}{\partial \xi} = 0, \quad \text{for } 0 \le \eta \le 1, \\ \dfrac{\partial^2 T_{s1}}{\partial \eta^2} - \dfrac{Pe}{2\phi}\dfrac{\partial T_{s0}}{\partial \omega_1} = 0, \quad \text{for } 1 \le \eta \le \dfrac{1}{\varepsilon}, \\ T_{s1}\Big|_{\eta=1} = T_{f1}\Big|_{\eta=1}, \quad \dfrac{\partial T_{f1}}{\partial \eta}\Big|_{\eta=1} = \beta \dfrac{\partial T_{s1}}{\partial \eta}\Big|_{\eta=1}, \\ \dfrac{\partial T_{f1}}{\partial \eta}\Big|_{\eta=0} = 0, \quad \dfrac{\partial T_{s1}}{\partial \eta}\Big|_{\eta=\frac{1}{\varepsilon}} = 0. \end{cases}$$

At level σ^2:

$$\begin{cases} \dfrac{\partial^2 T_{f2}}{\partial \eta^2} - \dfrac{Pe}{2}\dfrac{\partial T_{f1}}{\partial \omega_1} - \dfrac{3Pe}{4}\left(1-\eta^2\right)\dfrac{\partial T_{f1}}{\partial \xi} - \dfrac{\partial T_{f0}}{\partial \omega_2} + \dfrac{\partial^2 T_{f0}}{\partial \xi^2} = 0, \quad \text{for } 0 \le \eta \le 1, \\ \dfrac{\partial^2 T_{s2}}{\partial \eta^2} - \dfrac{Pe}{2\phi}\dfrac{\partial T_{s1}}{\partial \omega_1} - \dfrac{1}{\phi}\dfrac{\partial T_{s0}}{\partial \omega_2} + \dfrac{\partial^2 T_{s0}}{\partial \xi^2} = 0, \quad \text{for } 1 \le \eta \le \dfrac{1}{\varepsilon}, \\ T_{s2}\Big|_{\eta=1} = T_{f2}\Big|_{\eta=1}, \quad \dfrac{\partial T_{f2}}{\partial \eta}\Big|_{\eta=1} = \beta \dfrac{\partial T_{s2}}{\partial \eta}\Big|_{\eta=1}, \\ \dfrac{\partial T_{f2}}{\partial \eta}\Big|_{\eta=0} = 0, \quad \dfrac{\partial T_{s2}}{\partial \eta}\Big|_{\eta=\frac{1}{\varepsilon}} = 0. \end{cases}$$

At level σ^3

$$\begin{cases} \dfrac{\partial^2 T_{f3}}{\partial \eta^2} - \dfrac{Pe}{2}\dfrac{\partial T_{f2}}{\partial \omega_1} - \dfrac{3Pe}{4}\left(1-\eta^2\right)\dfrac{\partial T_{f2}}{\partial \xi} - \dfrac{\partial T_{f1}}{\partial \omega_2} + \dfrac{\partial^2 T_{f1}}{\partial \xi^2} = 0, \quad \text{for } 0 \le \eta \le 1, \\ \dfrac{\partial^2 T_{s3}}{\partial \eta^2} - \dfrac{Pe}{2\phi}\dfrac{\partial T_{s2}}{\partial \omega_1} - \dfrac{1}{\phi}\dfrac{\partial T_{s1}}{\partial \omega_2} + \dfrac{\partial^2 T_{s1}}{\partial \xi^2} = 0, \quad \text{for } 1 \le \eta \le \dfrac{1}{\varepsilon}, \\ T_{s3}\Big|_{\eta=1} = T_{f3}\Big|_{\eta=1}, \quad \dfrac{\partial T_{f3}}{\partial \eta}\Big|_{\eta=1} = \beta \dfrac{\partial T_{s3}}{\partial \eta}\Big|_{\eta=1}, \\ \dfrac{\partial T_{f3}}{\partial \eta}\Big|_{\eta=0} = 0, \quad \dfrac{\partial T_{s3}}{\partial \eta}\Big|_{\eta=\frac{1}{\varepsilon}} = 0. \end{cases}$$

…

To solve the original set of equations, Eqs. (17) to (20), we must solve the above hierarchy of sets of equations, level by level. Obviously the solution at level σ^0 is:

$$T_{f0} \equiv T_{s0} = F_0\left(\omega_1, \omega_2, \xi\right), \tag{23}$$

which suggests that the terms T_{f0} and T_{s0} are always equal and independent of the coordinate η.

Based on Eq. (23), we next solve the equation set at level σ^1:

$$T_{f1} = \frac{Pe\left(\beta - \beta\varepsilon + \phi\varepsilon\right)}{16\phi\varepsilon}\frac{\partial F_0}{\partial \omega_1}\eta^4 - \frac{Pe\left(3\beta - 3\beta\varepsilon + \phi\varepsilon\right)}{8\phi\varepsilon}\frac{\partial F_0}{\partial \omega_1}\eta^2 + F_1\left(\omega_1, \omega_2, \xi\right), \tag{24}$$

$$T_{s1} = \frac{Pe}{4\phi}\frac{\partial F_0}{\partial \omega_1}\eta^2 - \frac{Pe}{2\phi\varepsilon}\frac{\partial F_0}{\partial \omega_1}\eta + F_1\left(\omega_1, \omega_2, \xi\right) + \frac{Pe\left(8 - 5\beta + 5\beta\varepsilon - 4\varepsilon - \phi\varepsilon\right)}{16\phi\varepsilon}\frac{\partial F_0}{\partial \omega_1} \tag{25}$$

Again, the function F_1 does not depend upon η.

Repeating the above procedure, we obtain more complicated results involving functions $F_2\left(\omega_1, \omega_2, \xi\right)$, $F_3\left(\omega_1, \omega_2, \xi\right)$, … Knowledge of the initial condition and boundary conditions at the entrance of the system is required to fully determine these functions. Although they are not explicitly known, these functions are known to be independent of η. Therefore, upon treating the η-free functions F_0, F_1, F_2, … as parameters, the dependence of T_{f0}, T_{f1}, T_{f2}, … and T_{s0}, T_{s1}, T_{s2}, … upon η is clearly specified.

Fortunately, the relative effective dispersivity can be evaluated with incomplete solutions at levels σ^0 and σ^1 only, owing to the rapid convergence of the expansions in Eqs. (21) and (22).

Substitution of Eq. (1) into Eq. (14) leads to:

$$\frac{a_{eff}}{a_f} = 1 + \frac{\varepsilon Pe}{4}\frac{3\int_0^1 \eta^2 T_f d\eta - \int_0^1 T_f d\eta}{\sigma\dfrac{\partial}{\partial \xi}\int_0^1 T_f d\eta}. \tag{26}$$

and upon making use of Eqs. (21) and (26), we obtain:

$$\frac{a_{eff}}{a_f} = 1 + \frac{\varepsilon Pe}{4}\frac{\dfrac{Pe\left(-9\beta + 9\beta\varepsilon - 2\phi\varepsilon\right)}{105\phi\varepsilon}\dfrac{\partial F_0}{\partial \omega_1} + O\left(\sigma\right)}{\dfrac{-\beta + \beta\varepsilon - \phi\varepsilon}{\phi\varepsilon}\dfrac{\partial F_0}{\partial \omega_1} + O\left(\sigma\right)}, \tag{27}$$

The infinitesimal $O\left(\sigma\right)$ can be ignored as $\sigma = \dfrac{H}{L}$ is small, resulting in:

$$\frac{a_{eff}}{a_f} = 1 + CPe^2, \text{ and} \tag{28}$$

$$C = \frac{\varepsilon}{420}\frac{9\beta - 9\beta\varepsilon + 2\phi\varepsilon}{\beta - \beta\varepsilon + \phi\varepsilon} = \frac{\varepsilon}{420}\frac{9\left(1-\varepsilon\right)\rho_s c_s + 2\varepsilon\rho_f c_{pf}}{\left(1-\varepsilon\right)\rho_s c_s + \varepsilon\rho_f c_{pf}}. \tag{29}$$

In Eq. (28), the first term of unity on the right hand side represents the classical molecular conductivity, whilst the second term gives the effect of thermal dispersion. This is consistent with a previous observation by Kaviany [20]: if an idealized porous medium has in-line arrangement a Pe^2 relationship exists, whereas for stagger arrangement or randomized porous structures, the power index tends to unity.

The analytical results of Eqs. (28) and (29) demonstrate that the dispersion effect is always proportional to Pe^2 for the parallel plate array model, no matter how the thermal disturbance is introduced and how the initial temperature is distributed. The constant C is dependent upon both the structural porosity ε and upon the effective heat capacity ratio $\frac{\rho_s c_s}{\rho_f c_f}$; this dependence is plotted in Fig. 4. In the limit $\varepsilon = 1$ (i.e. the plates have zero-thickness), the relative effective dispersivity of (34) reduces to:

$$\frac{a_{eff}}{a_f} = 1 + \frac{1}{210}Pe^2, \tag{30}$$

which agrees with the result given by Kurzweg and Jaeger [4].

5. Steady heat transfer across an array of parallel plates

In the absence of thermal pulses, the steady state transfer of heat occurs across an array of parallel plates if steady heat sources are embedded within the plates. In this section, three selected cases are studied and analytical solutions for temperature distributions are obtained:

(1) Plates of zero thickness and constant heat flux, q, flowing from plate surfaces into the neighboring fluid channels;

(2) Plates of zero thickness and constant temperature, T_w, at the plate surfaces;

(3) Plates of finite thickness and uniform heat density, $\dot{Q}$.

5.1. Zero-thickness plate with constant heat flux

If the solid plates have zero thickness (i.e. $D = H$), the problem is considerably simplified because the volume averaging is performed on the fluid phase only. Thermal dispersion persists within the array of zero-thickness plates due to the non-uniformity of local fluid velocity.

For this case, Eq. (2) is unnecessary and Eq. (3) can be re-written, with the unsteady term omitted, as:

$$\frac{\partial\left(uT\right)}{\partial x} = a_f\left(\frac{\partial^2 T}{\partial x^2} + \frac{\partial^2 T}{\partial y^2}\right). \tag{31}$$

Also, Eq. (12) becomes:

$$u_{av}\frac{d\left\langle T\right\rangle}{dx} = a_{eff}\frac{d^2\left\langle T\right\rangle}{dx^2} + \frac{q}{d\rho_f c_f}, \tag{32}$$

where the heat flux q comes from the homogenization of constant heat flux boundary condition. The internal heat source density $\dot{Q}$ becomes singular as the thickness of place closes to be zero, in order to maintain a constant heat flux.

Substituting $T = \left\langle T\right\rangle + T'$ and $u = \left\langle u\right\rangle + u'$ into Eq. (31) and taking the y-direction averaging, we arrive at:

$$u_{av}\frac{d\left\langle T\right\rangle}{dx} + \frac{d\left\langle u'T'\right\rangle}{dx} = a_f\frac{d^2\left\langle T\right\rangle}{dx^2} + \frac{a_f q}{kD}. \tag{33}$$

Alternatively, Eq. (33) can be written in a form similar to Eq. (32):

$$u_{av}\frac{d\left\langle T\right\rangle}{dx} = a_f\frac{d^2\left\langle T\right\rangle}{dx^2} - \frac{d\left\langle u'T'\right\rangle}{dx} + \frac{q}{\rho_f c_f D} \tag{34}$$

Upon comparing Eqs. (32) and (34), we have:

$$a_{eff}\frac{d\langle T\rangle}{dx}=a_f\frac{d\langle T\rangle}{dx}-\langle u'T'\rangle, \text{ or} \tag{35}$$

$$k_{eff}\frac{d\langle T\rangle}{dx}=k_f\frac{d\langle T\rangle}{dx}-\rho_f c_f\left(\langle uT\rangle-\langle u\rangle\langle T\rangle\right). \tag{36}$$

from which we obtain:

$$\frac{k_{eff}}{k_f}=1+\frac{1}{a_f}\frac{\langle u\rangle\langle T\rangle-\langle uT\rangle}{d\langle T\rangle/dx}. \tag{37}$$

The analytical solution for the temperature field in the array is given by (see Appendix B):

$$T=\frac{2q}{k_f Pe}x-\frac{q}{8k_f H^3}y^4+\frac{3q}{4k_f H}y^2+T_0, \tag{38}$$

where T_0 is the reference temperature at the origin of the coordinate system. It follows from (43) that the stream-wise temperature gradient is constant. This gradient is proportional to the heat source density and inversely proportional to the average fluid velocity, fluid heat capacity and distance between plates.

Substitution of Eqs. (1) and (38) into Eq. (37) results in:

$$\frac{k_{eff}}{k_f}=1+\frac{3}{140}Pe^2. \tag{39}$$

Again, it is seen that the relative effective dispersivity has the form of $1+CPe^2$, with $C=\frac{3}{140}$.

5.2. Constant wall temperature boundary conditions

For zero-thickness plates, we again have $D=H$. Upon assuming that the solid plates have constant surface temperature, T_w, we obtain the analytical solution for temperature field (see Appendix C):

$$T = T_w - \theta\left(T_w - T_m\right) = T_w - \theta \Delta T_0 e^{-\frac{Nu}{Pe}\frac{x}{H}}, \tag{40}$$

where ΔT_0 is the difference between wall temperature and centerline temperature at the entrance, and θ is the dimensionless excess temperature determined from:

$$\frac{d^2\theta}{d\eta^2} + \theta\left(-\frac{3Nu}{4}\eta^2 + \frac{3Nu}{4} + \frac{Nu^2}{Pe^2}\right) = 0. \tag{41}$$

Here, η is the dimensionless coordinate in the cross-stream direction and the associated boundary conditions are given by:

$$\theta\Big|_{\eta=1} = 0, \quad \left.\frac{d\theta}{d\eta}\right|_{\eta=1} = -\frac{Nu}{2}, \quad \left.\frac{d\theta}{d\eta}\right|_{\eta=0} = 0. \tag{42}$$

As discussed in Appendix C, the solution to Eq. (41) subjected to the conditions of (42) is an even function of Pe.

With the above solutions to the temperature field, the effective dispersivity of the parallel-plate array system is given by:

$$\frac{k_{eff}}{k_f} = 1 + Pe^2\,\frac{1 - \int_0^1 \theta d\eta}{2Nu}. \tag{43}$$

This can be rewritten as $1 + CPe^2$, where

$$C = \frac{1}{2Nu} - \frac{1}{2Nu}\int_0^1 \theta d\eta \tag{44}$$

depends upon the solution of Eq. (41). Now, Eq. (41) is a non-linear second-order ordinary differential equation, and possesses a closed-form solution (see Appendix C). As the Peclet number Pe is a free variable in Eq. (41), the coefficient C is no longer constant; instead it is a function of Pe. Fig. 5 plots the relatively effective dispersivity k_{eff}/k_f as a function of Pe, whilst the dependence of C on Pe is shown in Fig. 6. It is seen from these results that the term $\frac{Nu^2}{Pe^2}$ in Eq. (41) is significant only if the Peclet

number is relatively small ($Pe < 20$). When $Pe \geq 20$, $k_{eff} \,/\, k_f$ has the usual Pe dependence, and C asymptotes to a constant (Fig. 6).

In order to evaluate the limiting value of C , we ignore the term $\dfrac{Nu^2}{Pe^2}$ in Eq. (41) to arrive at:

$$\frac{d^2\theta}{d\eta^2} + \theta\left(-\frac{3Nu}{4}\eta^2 + \frac{3Nu}{4}\right) = 0\,. \tag{45}$$

Solving C from Eqs. (44) and (45), we obtain $C = 0.02426$. Consequently, for usual Peclet numbers ($Pe \geq 20$), the relatively effective dispersivity can be written as:

$$\frac{k_{eff}}{k_f} = 1 + 0.02426Pe^2\,. \tag{46}$$

This limiting value of C is included in Fig. 6.

5.3. Constant heat flux boundary conditions with finite plate thickness

The last case analyzed is an array of parallel plates having finite thickness and uniform heat density, $\dot{Q}$. The heat fluxes on all plate surfaces have a single constant value. The situation is similar to Case 1 discussed in Section 5.1 and hence can be solved by following the same procedure. With some additional effort, the analytical solution for the temperature field is obtained as:

$$T_f = \frac{\dot{Q}\left(D-H\right)}{2Pek_f}x - \frac{\dot{Q}\left(D-H\right)}{8k_fH^3}y^4 + \frac{3\dot{Q}\left(D-H\right)}{4k_fH}y^2 + T_0\,, \text{ for } \left|y\right| \leq H\,, \tag{47}$$

$$T_s = \frac{\dot{Q}\left(D-H\right)}{2Pek_f}x - \frac{\dot{Q}}{2k_s}y^2 + \frac{\dot{Q}D}{k_s}y + T_0 + \frac{\dot{Q}DH}{k_s}\left[\frac{5}{8}\beta\left(1-\varepsilon\right) - 1 + \frac{\varepsilon}{2}\right] \quad , \quad \text{for}$$

$$H \leq \left|y\right| \leq D \tag{48}$$

With the above temperature field, the relative effective dispersivity is finally obtained as:

$$\frac{k_{eff}}{k} = 1 + \frac{3\varepsilon}{140} Pe^2 . \qquad (49)$$

The relationship of $1 + CPe^2$ appears again, where $C = \frac{3\varepsilon}{140}$ is independent of Pe.

Note that, when $\varepsilon = 1$, the relationship of (49) reduces to Eq. (39) for an array of parallel plates with zero thickness. In other words, Case 1 discussed in Section 5.1 is just a limiting case of that discussed in this section.

6. Discussion

The analytical results presented in this paper for various cases of the parallel-plate model clearly demonstrate that the effective thermal dispersivity of the system varies with thermal setting. The effect of thermal dispersion for the transient case differs from that for the steady case. Even for the steady case, the dispersion is different when the boundary types are different. For each case considered, the thermal dispersion depends only on structure properties and the underlying flow; changes in initial thermal conditions do not change the dispersion.

In the limiting case when the solid plates have zero thickness ($\varepsilon = 1$), the effective thermal dispersivity is plotted in Fig. 5 as a function of the Peclet number for both steady and transient heat transfer. For a given Peclet number, the results of Fig. 5 show that the constant wall temperature boundary condition has the maximal dispersion effect whilst the transient case has the minimal effect. This is because: (a) all three cases have identical velocity non-uniformity; (b) for the transient case, the temperature non-uniformity is only caused by the underlying velocity non-uniformity, thus has the minimal degree of temperature non-uniformity; (c) for the constant heat flux and constant wall temperature conditions, in addition to the temperature non-uniformity due to velocity non-uniformity, the artificially imposed heat source condition also contributes to the temperature non-uniformity. Furthermore, the boundary condition of a constant wall temperature enhances the temperature non-uniformity to more than that

of the constant heat flux case. This may be attributed to the fact that the input energy needed to maintain a constant wall temperature is more than that needed to maintain a constant heat flux.

Note that Eq. (28) can be transformed into Eq. (49) when the solid to fluid heat capacity ratio, $\rho_s c_s / \rho_f c_{pf}$, becomes infinitely large. This is reasonable by the following reasoning. When the heat capacity of the solid is much larger than that of the fluid, the thermal status of a solid plate is resistant to temperature changes in the neighboring fluid phase, and hence the heat flux from the solid plate approaches a constant.

7. Conclusions

The analytical results using the parallel plate array model lead to the following conclusions.

(1) Thermal dispersion in a porous medium such as parallel plate arrays is caused by the non-uniformity of heat flux distribution at the pore (microscopic) level. This includes both velocity non-uniformity and temperature non-uniformity. Temperature non-uniformity is caused either by velocity non-uniformity or by different thermal boundary settings.

(2) The effective thermal dispersivity of a porous medium has contributions from both the molecular diffusion and hydraulic dispersion. In the parallel plate array model, the hydraulic dispersion is always proportional to Pe^2 and quickly surpasses the molecular diffusion as the Peclet number increases, becoming the dominant mechanism for heat transfer.

(3) Thermal dispersion is ***not*** a property of the porous medium depending only on the pore morphology, porosity and the underlying fluid flow. It is also affected by the type of thermal setting imposed on the medium. This is because the velocity non-uniformity is not the only cause of temperature non-uniformity. Different thermal boundary types also change the pore-level temperature non-uniformity, and hence the dispersion of heat. In other words, the effective

thermal dispersivity of a porous medium obtained using one type of thermal setting should be used cautiously when the thermal setting is changed.

(4) Under the condition that the solid heat capacity is much larger than that of the fluid, the case of constant heat source density in solid plates (i.e. the case discussed in Section 5.3) can be represented by the transient case (i.e. that discussed in Section 4). It can be further reduced to the case of constant heat flux when the porosity approaches unity (i.e., the plates have zero thickness, the case discussed in Section 5.1).

Acknowledgement

The authors wish to thank the UK Engineering and Physical Sciences Research Council (EPSRC), Overseas Research Students Awards Scheme (ORSAS) and Cambridge Overseas Trust for financial support of this work.

Appendix A. *Y*-direction averaging procedure and its characteristics

From the y-direction averaging described in Eq. (5), the following characteristics of the volume-averaged variables and the deviations can be obtained:

1) Averaged variables and deviation variables:

$$\Big\langle\Big\langle \boldsymbol{\Phi} \Big\rangle\Big\rangle = \frac{1}{2D}\int_{-D}^{D}\Big\langle \boldsymbol{\Phi} \Big\rangle dy = \frac{1}{2D}\Big\langle \boldsymbol{\Phi} \Big\rangle 2D = \Big\langle \boldsymbol{\Phi} \Big\rangle,$$

$$\Big\langle \boldsymbol{\Phi}' \Big\rangle = \frac{1}{2D}\int_{-D}^{D}\Big(\boldsymbol{\Phi} - \Big\langle \boldsymbol{\Phi} \Big\rangle\Big) dy = \frac{1}{2D}\int_{-D}^{D}\boldsymbol{\Phi} dy - \frac{1}{2D}\int_{-D}^{D}\Big\langle \boldsymbol{\Phi} \Big\rangle dy = \Big\langle \boldsymbol{\Phi} \Big\rangle - \Big\langle \boldsymbol{\Phi} \Big\rangle = 0\,,$$

$$\Big\langle \boldsymbol{\Phi} \Big\rangle' = \Big\langle \boldsymbol{\Phi} \Big\rangle - \Big\langle\Big\langle \boldsymbol{\Phi} \Big\rangle\Big\rangle = \Big\langle \boldsymbol{\Phi} \Big\rangle - \Big\langle \boldsymbol{\Phi} \Big\rangle = 0\,,$$

$$\boldsymbol{\Phi}'' = \boldsymbol{\Phi}' - \Big\langle \boldsymbol{\Phi}' \Big\rangle = \boldsymbol{\Phi}' - 0 = \boldsymbol{\Phi}' \quad .$$

In summary,

$$\Big\langle\Big\langle \boldsymbol{\Phi} \Big\rangle\Big\rangle = \Big\langle \boldsymbol{\Phi} \Big\rangle,\ \Big\langle \boldsymbol{\Phi}' \Big\rangle = 0\,,\ \Big\langle \boldsymbol{\Phi} \Big\rangle' = 0\,,\ \boldsymbol{\Phi}'' = \boldsymbol{\Phi}'; \tag{A1}$$

2) Summation and product of two variables:

$$\Big\langle \boldsymbol{\Phi}_1 + \boldsymbol{\Phi}_2 \Big\rangle = \frac{1}{2d}\int_{-d}^{d}\Big(\boldsymbol{\Phi}_1 + \boldsymbol{\Phi}_2\Big) dy = \frac{1}{2D}\int_{-D}^{D}\boldsymbol{\Phi}_1 dy + \frac{1}{2D}\int_{-D}^{D}\boldsymbol{\Phi}_2 dy = \Big\langle \boldsymbol{\Phi}_1 \Big\rangle + \Big\langle \boldsymbol{\Phi}_2 \Big\rangle,$$

$$\begin{aligned}
\Big\langle \boldsymbol{\Phi}_1\boldsymbol{\Phi}_2 \Big\rangle &= \Big\langle\Big(\Big\langle \boldsymbol{\Phi}_1 \Big\rangle + \boldsymbol{\Phi}_1'\Big)\Big(\Big\langle \boldsymbol{\Phi}_2 \Big\rangle + \boldsymbol{\Phi}_2'\Big)\Big\rangle = \Big\langle\Big\langle \boldsymbol{\Phi}_1 \Big\rangle\Big\langle \boldsymbol{\Phi}_2 \Big\rangle + \boldsymbol{\Phi}_1'\boldsymbol{\Phi}_2' + \Big\langle \boldsymbol{\Phi}_1 \Big\rangle\boldsymbol{\Phi}_2' + \boldsymbol{\Phi}_1'\Big\langle \boldsymbol{\Phi}_2 \Big\rangle\Big\rangle \\
&= \Big\langle\Big\langle \boldsymbol{\Phi}_1 \Big\rangle\Big\langle \boldsymbol{\Phi}_2 \Big\rangle\Big\rangle + \Big\langle \boldsymbol{\Phi}_1'\boldsymbol{\Phi}_2' \Big\rangle + \Big\langle\Big\langle \boldsymbol{\Phi}_1 \Big\rangle\boldsymbol{\Phi}_2' \Big\rangle + \Big\langle \boldsymbol{\Phi}_1'\Big\langle \boldsymbol{\Phi}_2 \Big\rangle\Big\rangle \\
&= \Big\langle \boldsymbol{\Phi}_1 \Big\rangle\Big\langle \boldsymbol{\Phi}_2 \Big\rangle + \Big\langle \boldsymbol{\Phi}_1'\boldsymbol{\Phi}_2' \Big\rangle + \Big\langle \boldsymbol{\Phi}_1 \Big\rangle\Big\langle \boldsymbol{\Phi}_2' \Big\rangle + \Big\langle \boldsymbol{\Phi}_1' \Big\rangle\Big\langle \boldsymbol{\Phi}_2 \Big\rangle \\
&= \Big\langle \boldsymbol{\Phi}_1 \Big\rangle\Big\langle \boldsymbol{\Phi}_2 \Big\rangle + \Big\langle \boldsymbol{\Phi}_1'\boldsymbol{\Phi}_2' \Big\rangle + \Big\langle \boldsymbol{\Phi}_1 \Big\rangle\bullet 0 + 0\bullet\Big\langle \boldsymbol{\Phi}_2 \Big\rangle \\
&= \Big\langle \boldsymbol{\Phi}_1 \Big\rangle\Big\langle \boldsymbol{\Phi}_2 \Big\rangle + \Big\langle \boldsymbol{\Phi}_1'\boldsymbol{\Phi}_2' \Big\rangle
\end{aligned} \quad .$$

In summary,

$$\Big\langle \boldsymbol{\Phi}_1 + \boldsymbol{\Phi}_2 \Big\rangle = \Big\langle \boldsymbol{\Phi}_1 \Big\rangle + \Big\langle \boldsymbol{\Phi}_2 \Big\rangle,\ \Big\langle \boldsymbol{\Phi}_1\boldsymbol{\Phi}_2 \Big\rangle = \Big\langle \boldsymbol{\Phi}_1 \Big\rangle\Big\langle \boldsymbol{\Phi}_2 \Big\rangle + \Big\langle \boldsymbol{\Phi}_1'\boldsymbol{\Phi}_2' \Big\rangle; \tag{A2}$$

3) Derivatives:

$$\left\langle \frac{\partial \boldsymbol{\Phi}}{\partial x} \right\rangle = \frac{1}{2D}\int_{-D}^{D} \frac{\partial \boldsymbol{\Phi}}{\partial x} dy = \frac{1}{2D}\int_{-D}^{D} \lim_{\delta x \to 0} \frac{\boldsymbol{\Phi}\left(x+\delta x, y\right) - \boldsymbol{\Phi}\left(x, y\right)}{\delta x} dy$$

$$= \lim_{\delta x \to 0} \frac{\frac{1}{2D}\int_{-D}^{D} \boldsymbol{\Phi}\left(x+\delta x, y\right) dy - \frac{1}{2D}\int_{-D}^{D} \boldsymbol{\Phi}\left(x, y\right) dy}{\delta x} = \frac{\partial}{\partial x}\left(\frac{1}{2D}\int_{-D}^{D} \boldsymbol{\Phi} dy\right) = \frac{\partial \left\langle \boldsymbol{\Phi} \right\rangle}{\partial x}$$

.

Similarly,

$$\left\langle \frac{\partial^2 \boldsymbol{\Phi}}{\partial x^2} \right\rangle = \frac{\partial}{\partial x}\left\langle \frac{\partial \boldsymbol{\Phi}}{\partial x} \right\rangle = \frac{\partial}{\partial x}\left(\frac{\partial \left\langle \boldsymbol{\Phi} \right\rangle}{\partial x}\right) = \frac{\partial^2 \left\langle \boldsymbol{\Phi} \right\rangle}{\partial x^2}.$$

To summarise, we have

$$\left\langle \frac{\partial \boldsymbol{\Phi}}{\partial x} \right\rangle = \frac{\partial \left\langle \boldsymbol{\Phi} \right\rangle}{\partial x}, \left\langle \frac{\partial^2 \boldsymbol{\Phi}}{\partial x^2} \right\rangle = \frac{\partial^2 \left\langle \boldsymbol{\Phi} \right\rangle}{\partial x^2}. \tag{A3}$$

4) Overall volume-averaging and intrinsic volume-averaging:

$$\left\langle \Phi \right\rangle = \varepsilon \left\langle \Phi \right\rangle^f = \left(1-\varepsilon\right)\left\langle \Phi \right\rangle^s, \tag{A4}$$

where $\varepsilon = H/D$ is the porosity of the parallel plate array.

Appendix B. Analytical solution for constant heat-flux boundary condition

In the fully developed region for heat transfer, the local heat transfer coefficient is constant along the stream-wise direction. For the present problem, the local heat transfer coefficient, h_x, along the plate surface is given by:

$$h_x = \frac{-q}{T_{m,x} - T_{w,x}}, \tag{B1}$$

Where $T_{w,x}$ and $T_{m,x}$ are the local values of the plate surface temperature and bulk-mean fluid temperature, respectively. The bulk-mean fluid temperature is defined as:

$$T_m = \frac{\int_{-H}^{H} \left(uT\right) dy}{\int_{-H}^{H} u dy}. \tag{B2}$$

Since $h_x = h$ is constant along the x-direction, $T_{m,x} - T_{w,x}$ is also independent of x. This implies that the temperature difference between fluid (bulk-mean) and wall is constant if the wall heat flux is constant and the flow is fully developed, namely:

$$T_m - T_w = -\frac{q}{h} \tag{B3}$$

Let the dimensionless excess temperature be defined as:

$$\theta\left(x, y\right) = \frac{T - T_w}{T_m - T_w}, \tag{B4}$$

The boundary conditions can then be written as:

$$\theta\Big|_{y=\pm H} = 0,$$

$$\left.\frac{\partial \theta}{\partial y}\right|_{y=\pm H} = \mp \frac{h}{k}.$$

For fully developed laminar convection, substitution of Eq. (1) into Eq. (B2) leads to:

$$T_m = \frac{3}{4b} \int_{-H}^{H} \left[\left(1 - \frac{y^2}{H^2}\right) T\right] dy. \tag{B5}$$

From Eqs. (B3) and (B4), we have

$$T = -\frac{q}{h}\theta + T_w. \tag{B6}$$

Substituting Eq. (B6) into Eq. (B5), we have

$$T_m = \frac{3q}{4hH} \int_{-H}^{H} \left[\left(1 - \frac{y^2}{H^2}\right) \theta\right] dy + T_w, \tag{B7}$$

and, because of Eq. (B3),

$$\frac{1}{2H} \int_{-H}^{H} \left[\left(1 - \frac{y^2}{H^2}\right) \theta\right] dy = \frac{2}{3}. \tag{B8}$$

Since the right-hand side of Eq. (B8) is a constant, the left-hand side should not depend on x. Hence θ must be independent of x, that is,

$$\frac{\partial \theta}{\partial x} = 0. \tag{B9}$$

Making use of Eqs. (B3), (B6) and (B9), we arrive at:

$$\frac{\partial T}{\partial x} = \frac{dT_m}{dx} = \frac{dT_w}{dx}. \tag{B10}$$

This means that, at any given position along the cross-stream direction, the stream-wise temperature gradient remains unchanged in the stream-wise direction (i.e. $\partial T / \partial x$ does not depend on y).

Considerations of energy conservation for a volume shown by dashed lines in Fig. 7 lead to:

$$kH \frac{d^2 T_m}{dx^2} - \rho c_p u_m H \frac{dT_m}{dx} = q. \tag{B11}$$

Note that Eq. (B10) has been used to account for the net energy increase due to conduction. Eq. (B11) is a nonhomogeneous ordinary linear differential equation of the second order; its general solution is of the form:

$$T_b = C_1 + C_2 e^{\frac{u_m}{a}x} + \frac{aq}{ku_m H} x, \tag{B12}$$

where C_1 and C_2 are constants to be determined, and $a = k / \rho c$.

The net energy increase due to stream-wise conduction can be written as:

$$E_{cond} = kH \frac{d^2 T_m}{dx^2} = C_2 kH \frac{u_m^2}{a^2} e^{\frac{u_m}{a}x}, \tag{B13}$$

and that due to convection is given by:

$$E_{conv} = -\rho c_p u_m H \frac{dT_m}{dx} = -C_2 kH \frac{u_m^2}{a^2} e^{\frac{u_m}{a}x} - q. \tag{B14}$$

If $C_2 \neq 0$, we have the unrealistic situation that $\left|E_{cond}\right| \approx \left|E_{conv}\right|$ when x is sufficiently large. Therefore we must have $C_2 = 0$, and Eq. (B12) becomes:

$$T_b = C_1 + \frac{aq}{ku_m H} x. \tag{B15}$$

from which:

$$\frac{d\left\langle T\right\rangle}{dx}=\frac{aq}{ku_mH}=\frac{q}{\rho cu_mH}=\frac{2q}{kPe}. \tag{B16}$$

This means that the stream-wise temperature gradient $d\left\langle T\right\rangle/dx$ is constant in the fully developed region. The gradient is proportional to the heat source density of plates and inversely proportional to the average fluid velocity, the fluid heat capacity and the distance between plates.

Eqs. (B10) and (B16) suggest that the distribution of temperature in the channel has the form:

$$T=\frac{2q}{kPe}x+f\left(y\right). \tag{B17}$$

Substitution of Eq. (B17) into Eq. (1) leads to a second-order ordinary differential equation for function $f\left(y\right)$:

$$\frac{d^2f\left(y\right)}{dy^2}=\frac{3q}{2kH}\left(1-\frac{y^2}{H^2}\right). \tag{B18}$$

from which:

$$f\left(y\right)=-\frac{q}{8kH^3}y^4+\frac{3q}{4kH}y^2+C_3y+C_4. \tag{B19}$$

Due to symmetry in the y-direction, $C_3=0$, thus:

$$f\left(y\right)=-\frac{q}{8kH^3}y^4+\frac{3q}{4kH}y^2+C_4. \tag{B20}$$

Finally, the temperature field in the parallel plate array system is obtained as:

$$T=\frac{2q}{kPe}x-\frac{q}{8kH^3}y^4+\frac{3q}{4kH}y^2+C_4, \tag{B21}$$

where C_4 is a constant, and can be determined if the temperature at a given location is given. It can be checked that Eq. (B21) satisfies the governing equation and the boundary conditions.

Appendix C. Analytical solution for constant wall-temperature boundary conditions

Under constant wall-temperature boundary conditions, in the fully developed region for heat transfer, the local heat transfer coefficient, defined by Eq. (B1), and the stream-wise gradient of the dimensionless excess temperature, defined by Eq. (B4), are all constant. By energy conservation of the volume shown in Fig. 7:

$$h\left(T_w - T_m\right)dx = \rho c u_m H dT_m = -\rho c u_m H d\left(T_w - T_m\right) \tag{C1}$$

from which:

$$\frac{d\left(T_w - T_m\right)}{\left(T_w - T_m\right)} = -\frac{h}{\rho c u_m H}dx \tag{C2}$$

If follows immediately that:

$$\left(T_w - T_m\right) = C_5 e^{-\frac{h}{\rho c u_m H}x}, \tag{C3}$$

where the constant C_5 can be determined from the inlet condition (i.e., at $x = 0$), $T_w - T_{m,inlet} = \Delta T_0$. Eq. (C3) can be written as:

$$\left(T_w - T_m\right) = \Delta T_0 e^{-\frac{h}{\rho c u_m H}x}. \tag{C4}$$

Because of Eq. (B4), we have:

$$T = T_w - \theta\left(T_w - T_m\right) = T_w - \theta \Delta T_0 e^{-\frac{h}{\rho c u_m H}x}. \tag{C5}$$

where only θ is a function of the y-coordinate. Substitution of Eq. (C5) into Eq. (31) results in:

$$\frac{d^2\theta}{dy^2} + \theta\left(-\frac{3h}{2k_f H^3}y^2 + \frac{3h}{2k_f H} + \frac{h^2}{\rho_f^2 c_f^2 u_m^2 H^2}\right) = 0. \tag{C6}$$

Introducing the dimensionless coordinate as $\eta = \frac{y}{H}$ and remembering the definitions of Pe and Nu, we can rewrite Eq. (C6) as:

$$\frac{d^2\theta}{d\eta^2} + \theta\left(-\frac{3Nu}{4}\eta^2 + \frac{3Nu}{4} + \frac{Nu^2}{Pe^2}\right) = 0\,. \tag{C7}$$

Eq. (C7) is a linear second-order ordinary differential equation, with the Nusselt number Nu and Peclet number Pe appearing as parameters. If we can find the solution of Eq. (C7), we can determine the temperature field with Eq. (C5) and then evaluate thermal dispersion for constant wall temperature boundary conditions.

It can be shown that Eq. (B8) is also satisfied for constant wall temperature boundary conditions. Eq. (B8) can be written as:

$$\int_0^1 \left[\left(1-\eta^2\right)\theta\right] d\eta = \frac{2}{3}\,. \tag{C8}$$

The solution $\theta\left(\eta\right)$ of Eq. (C7) must also satisfy (C8). In addition, it should satisfy the force boundary condition:

$$\theta\Big|_{\eta=1} = 0\,. \tag{C9}$$

Furthermore, $\theta\left(\eta\right)$ must be an even function, i.e.:

$$\left.\frac{d\theta}{d\eta}\right|_{\eta=0} = 0\,, \tag{C10}$$

Finally, by definition, $\theta\left(\eta\right)$ must satisfy:

$$\left.\frac{d\theta}{d\eta}\right|_{\eta=1} = -\frac{Nu}{2}. \tag{C11}$$

Eq. (C7) has the form of the well-known Weber Differential Equation [22]. With the introduction of a new dimensionless variable $\zeta = \frac{1}{\sqrt[4]{3Nu}}\eta$, Eq. (C7) can be transformed to a standard form [23], as:

$$\frac{d^2\theta}{d\zeta^2} - \theta\left(\frac{1}{4}\zeta^2 + p\right) = 0\,, \tag{C12}$$

where

$$p = -\frac{\sqrt{3Nu}}{4} - \frac{\sqrt{Nu^3/3}}{Pe^2} < 0\,. \tag{C13}$$

The fundamental solutions to Eq. (C12) are the parabolic cylinder functions given below [24]:

$$\theta_1(\zeta) = e^{-\frac{\zeta^2}{4}} M\left(\frac{p}{2}+\frac{1}{4},\frac{1}{2};\frac{\zeta^2}{2}\right), \tag{C14a}$$

$$\theta_2(\zeta) = \zeta e^{-\frac{\zeta^2}{4}} M\left(\frac{p}{2}+\frac{3}{4},\frac{3}{2};\frac{\zeta^2}{2}\right), \tag{C14b}$$

where $M\left(a,b;x\right)$ is the Kummer's function of x with regard to parameters a and b [24]; θ_1 is an even function and θ_2 is an odd function. The general solution to Eq. (C12) is the linear combination of θ_1 and θ_2, $\theta = C_6\theta_1 + C_7\theta_2$. The integral constants, C_6 and C_7, are to be determined by the restriction conditions.

Firstly, $\theta\left(\zeta\right)$ remains as an even function after transformation from $\theta\left(\eta\right)$, and hence $C_7 = 0$, resulting in $\theta = C_6\theta_1$. With the integral constant C_6 renamed as A, the solution to Eq. (C7) is given by:

$$\theta\left(\eta\right) = A e^{-\frac{1}{4\sqrt{3Nu}}\eta^2} M\left(\frac{1}{4} - \frac{\sqrt{3Nu}}{8} - \frac{\sqrt{Nu^3}}{2\sqrt{3}Pe^2}, \frac{1}{2}; \frac{\eta^2}{2\sqrt{3Nu}}\right). \tag{C15}$$

From Eq. (C9), we have:

$$M\left(\frac{1}{4} - \frac{\sqrt{3Nu}}{8} - \frac{\sqrt{Nu^3}}{2\sqrt{3}Pe^2}, \frac{1}{2}; \frac{1}{2\sqrt{3Nu}}\right) = 0\,. \tag{C16}$$

If the Peclet number Pe is taken as a free parameter, (C16) suggests that the Nusselt number Nu is dependent upon Pe. For selected values of Pe, (C16) can be solved numerically. The solutions are listed in Table 1 and plotted in Fig. 8 as functions of Pe. Note that Nu approaches asymptotically the limit 3.78 as Pe is increased.

Next, the integral constant A is determined with Eq. (C8); the result is listed in Table 1 for different values of Pe. To emphasize the fact that both A and parameter Nu are dependent on Pe, the solution $\theta\left(\eta\right)$ is written as:

$$\theta\left(\eta\right)=A\left(Pe\right)e^{-\frac{1}{4\sqrt{3Nu\left(Pe\right)}}\eta^{2}}M\left(\frac{1}{4}-\frac{\sqrt{3Nu\left(Pe\right)}}{8}-\frac{\sqrt{\left(Nu\left(Pe\right)\right)^{3}}}{2\sqrt{3}Pe^{2}},\frac{1}{2};\frac{\eta^{2}}{2\sqrt{3Nu\left(Pe\right)}}\right) \tag{C17}$$

For $Pe=75$, we have $Nu=3.78$, $A=1.32044$, and the corresponding $\theta\left(\eta\right)$ is plotted in Fig. 9. Because $M\left(a,b;0\right)\equiv 1$, A denotes the amplitude factor of the dimensionless excess temperature at the fluid channel centre. For comparison, in Fig. 9, the dimensionless temperature distribution corresponding to other thermal settings is also shown.

To calculate the thermal dispersion we can substitute Eq. (C5) into Eq. (14) to show that the relative effective conductivity is again independent of x-coordinate and is given by:

$$\frac{k_{eff}}{k_f}=1+Pe^{2}\frac{1}{4Nu}\int_{0}^{1}\left[\left(1-3\eta^{2}\right)\theta\right]d\eta. \tag{C18}$$

From Eqs (C8) and (C18), we have:

$$\frac{k_{eff}}{k_f}=1+Pe^{2}\frac{1-\int_{0}^{1}\theta d\eta}{2Nu}. \tag{C19}$$

Apparently, the integral $\int_{0}^{1}\theta d\eta$ also depends on Pe. This is important because, in contrast with the constant heat flux case, we no longer have a simple relationship in the form of $1+CPe^{2}$ for the effective thermal diffusivity, as the coefficient C is no longer independent of Pe. To reiterate this, Eq. (C19) is written as:

$$\frac{k_{eff}}{k_f}=1+C\left(Pe\right)Pe^{2} \tag{C20}$$

$$C = \frac{1 - \int_0^1 \theta\left(Pe;\eta\right) d\eta}{2Nu\left(Pe\right)} \tag{C21}$$

The value of C as a function of Pe is plotted in Fig. 6.

References

[1] Taylor, G, 1953. Dispersion of soluble matter in solvent flowing slowly through a tube. *Proc. Roy. Soc*. Serial A (219): 86-203.

[2] Taylor, G, 1954. Conditions under which dispersion of a solute in a stream of solvent can be used to measure molecular diffusuion. *Proc. Roy. Soc*. Serial A (225): 473-477.

[3] Aris, R, 1956. On the dispersion of a solute in a fluid flowing through a tube. *Proc. Roy. Soc*. Serial A (235): 67-77.

[4] Kurzweg, G and Jaeger, 1997. *Int. J. Heat & Mass Transfer*, (1241): 1391-1400.

[5] Yuan Z G, Somerton, W H & Udell, K S, 1991. Thermal dispersion in the thick-walled tubes as a model of porous media. *Int. J. Heat Mass Transfer*. 34(11): 2715-2726.

[6] Batycky, R P, Edwards, D A & Brenner, H, 1993. Thermal Taylor dispersion in an insulated circular cylinder – T. Theory, II. Applications. *Int. J. Heat Mass Transfer*. 36: 4317-4333.

[7] Kuwahara, F, Nakayama, A & Koyama, H, 1996. A numerical study of thermal dispersion in porous media. *ASME J. Heat Transfer*, 118:756-761.

[8] Kuwahara, F & Nakayama, A, 1999. Numerical determination of thermal dispersion coefficients using a periodic porous structure. *ASME J. Heat Transfer*, 121:160-163.

[9] Nakayama, A & Kuwahara, F, 1999. A macroscopic turbulence model for flow in a porous medium. *J. Fluids Eng.*, 121: 427-433.

[10] Kuwahara, F, Shirota, M & Nakayama, A, 2001. A numerical study of interfacial convective heat transfer coefficients in two-energy equation model for convection in porous media. *Int. J. Heat Mass Transfer*, 44:1153-1159.

[11] Quintard, M, Kaviany, M & Whitaker, S, 1997. Two-medium treatment of heat transfer in porous media: numerical results for effective properties. *Adv. Water Resources*, 20(2,3): 77-94.

[12] Quintard, M and Whitaker, S, 1994. Local thermal equilibrium for transient heat conduction: theory and comparison with numerical experiments. *Int. J. Heat Mass Transfer*, 38: 2779-2796.

[13] Moyne, C, Didierjean, S, Amaral Souto, H P & da Silveira, O T, 2000. Thermal dispersion in porous media: one-equation model. *Int. J. Heat Mass Transfer*, 43: 3853-3867.

[14] Quintard, M & Whitaker, S, 1993. Transport in ordered and disordered porous media: Volume-averaged equations, closure problems and comparison with experiment. *Chem. Eng. Sci.*, 48: 2537-2564.

[15] Hsiao, K T & Advani, S G, 1999. A theory to describe heat transfer during laminar incompressible flow of a fluid in periodic porous media. *Phys. Fluids*, 11(7): 1738-1748.

[16] Whitaker, S, 1967. Diffusion and dispersion in porous media. *AIChE Journal*, 13(3): 420-427.

[17] Zanotti, F & Carbonell, R G, 1984. Development of transport equations for multiphase systems - I General development for two phase systems. *Chem. Eng. Sci.*, 39(2): 263-278.

[18] Zanotti, F & Carbonell, R G, 1984. Development of transport equations for multiphase systems - II Application to one-dimensional axi-symmetric flows of two phases. *Chem. Eng. Sci.*, 39(2): 279-297.

[19] Zanotti, F & Carbonell, R G, 1984. Development of transport equations for multiphase systems - III Application to heat transfer in packed beds. *Chem. Eng. Sci.*, 39(2): 299-311.

[20] Kaviany, M, 1995. Princinples of Heat Transfer in Porous Media, 2nd Ed. By Pringer.

[21] Incropera, F P & DeWitt, D P, 1985. Introduction to Heat Transfer, Pressed by John Wiley & Son, US.

[22] Weber differential equations. At http://mathworld.wolfram.com/WeberDifferentialEquations.html, June, 2004.

[23] Parabolic cylinder functions. At http://mathworld.wolfram.com/ParabolicCylinderFunction.html, June, 2004.

[24] Abramowitz, M & Stegum, I, 1964. Handbook of Mathematical Function with Formulas, Graphs and Mathematical Tables. Reprinted by Dover, New York.

Tables

Table 1 Values of Nu, A and C for constant wall temperature case and selected values of Pe

Pe	Nu	A	C
0.001	0.00157	1.29217	56.4032
0.01	0.0156	1.29268	5.63193
0.1	0.154	1.29370	0.578312
1.0	1.28	1.30220	0.702821
2.5	2.39	1.31048	0.380056
5.0	3.17	1.31597	0.0288198
7.5	3.46	1.31820	0.0264768
10.0	3.59	1.31932	0.0255592
15.0	3.69	1.31964	0.0248555
20.0	3.74	1.32015	0.0246123
30.0	3.77	1.32034	0.0244278
75.0	3.78	1.32044	0.0242925
750.0	3.78	1.32069	0.0242653

List of Figures

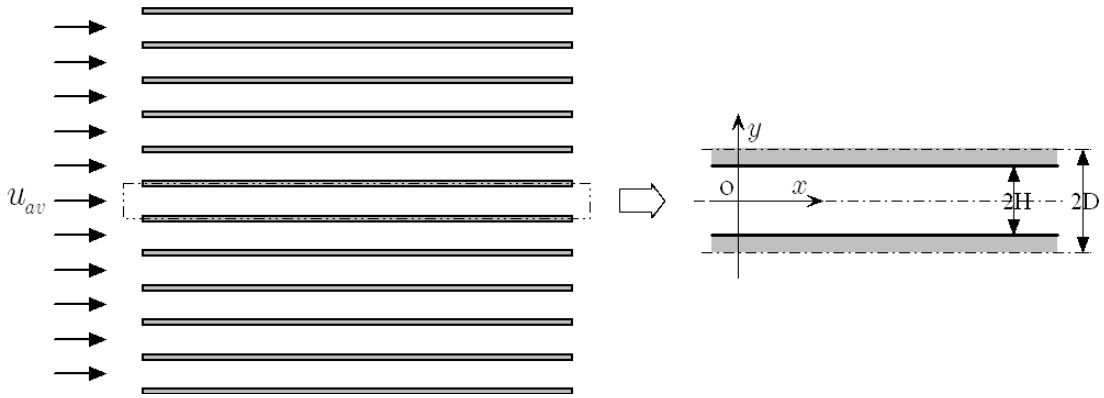

The focused domain is taken from fully developed region

Fig.1

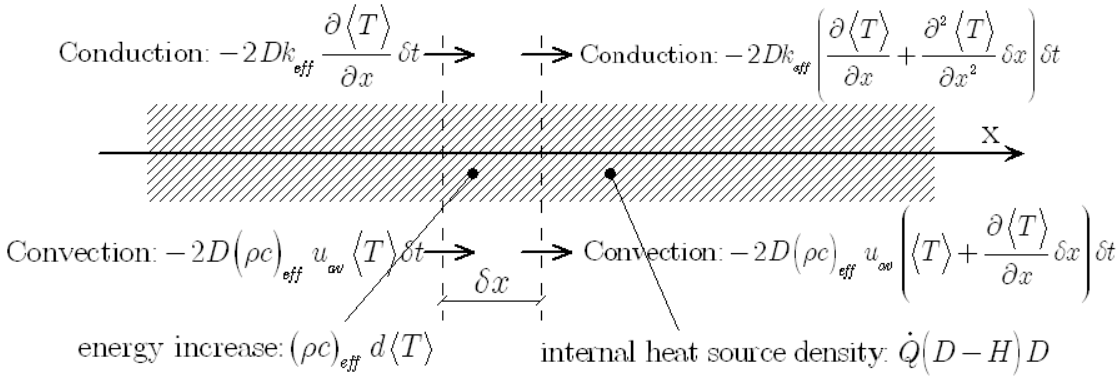

Energy balance analysis is for the macroscopic one-dimensional problem

Fig. 2

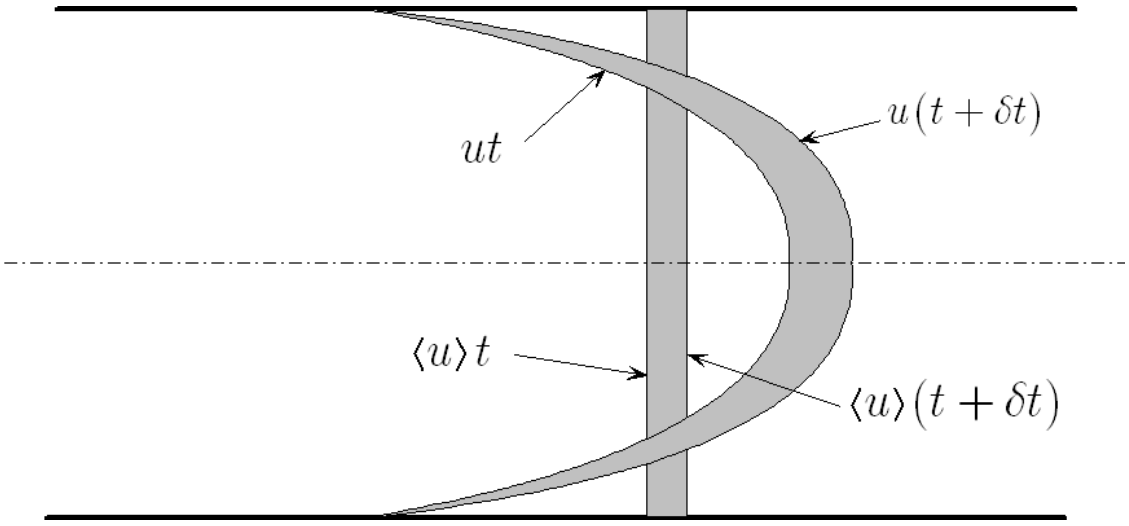

For time range from t to $t+\delta t$, the averaged fluid front moved from vertical line $\langle u\rangle t$ to line $\langle u\rangle(t+\delta t)$, whilst the real front actually moved from curved line ut to line $u(t+\delta t)$. The energy difference between the vertical bar and the curved grey area is $2H\rho_f c_f\left(\langle u\rangle\langle T\rangle-\langle uT\rangle\right)\delta t$.

Fig. 3

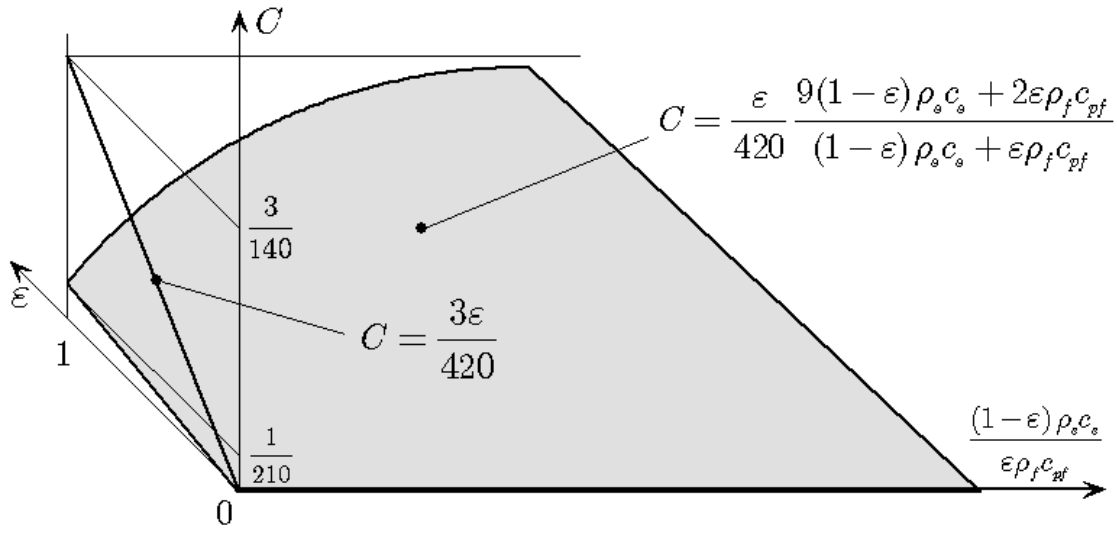

Fig. 4

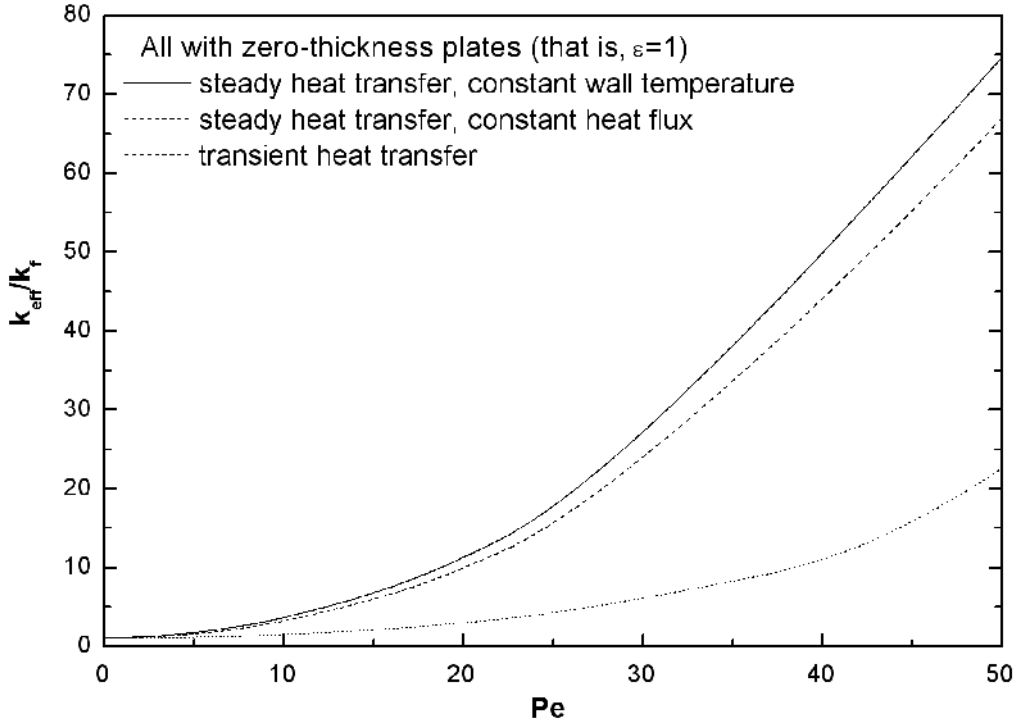
All with zero-thickness plates (that is, ε=1)
steady heat transfer, constant wall temperature
steady heat transfer, constant heat flux
transient heat transfer
k_{eff}/k_f
Pe
0
10
20
30
40
50
60
70
80

Fig. 5

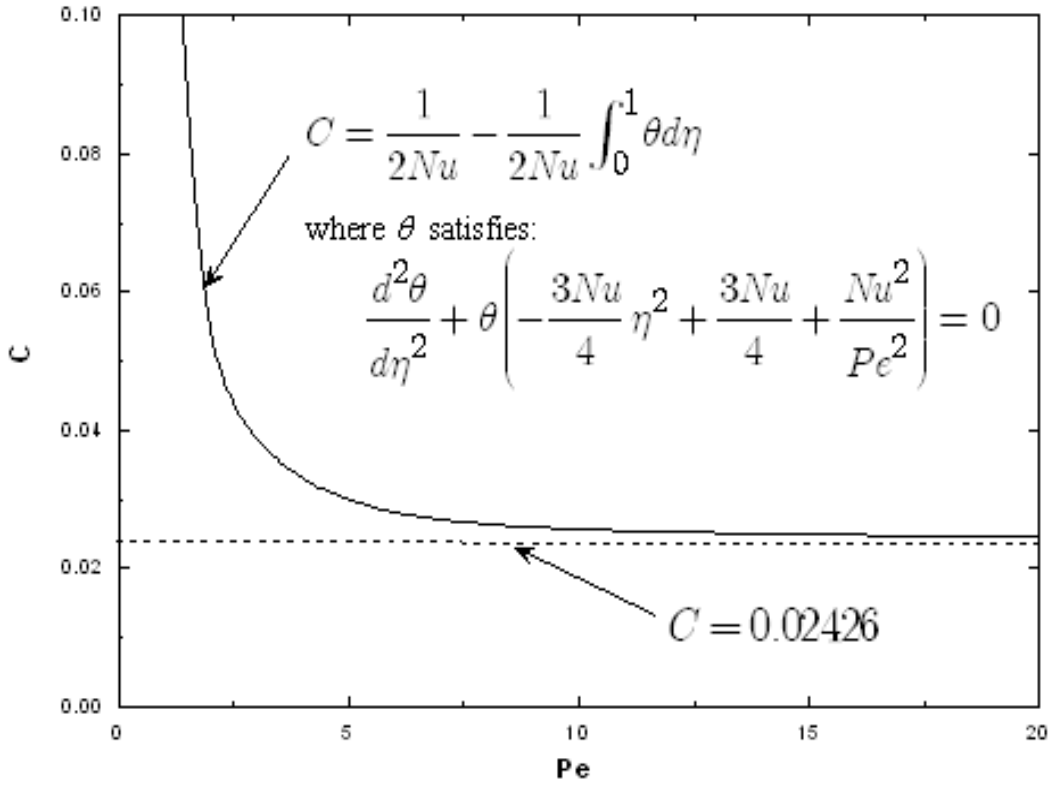
$C = \frac{1}{2Nu} - \frac{1}{2Nu}\int_0^1 \theta d\eta$
where θ satisfies:
$\frac{d^2\theta}{d\eta^2} + \theta\left(-\frac{3Nu}{4}\eta^2 + \frac{3Nu}{4} + \frac{Nu^2}{Pe^2}\right) = 0$
$C = 0.02426$
C
Pe
0.00
0.02
0.04
0.06
0.08
0.10
0
5
10
15
20

Fig. 6

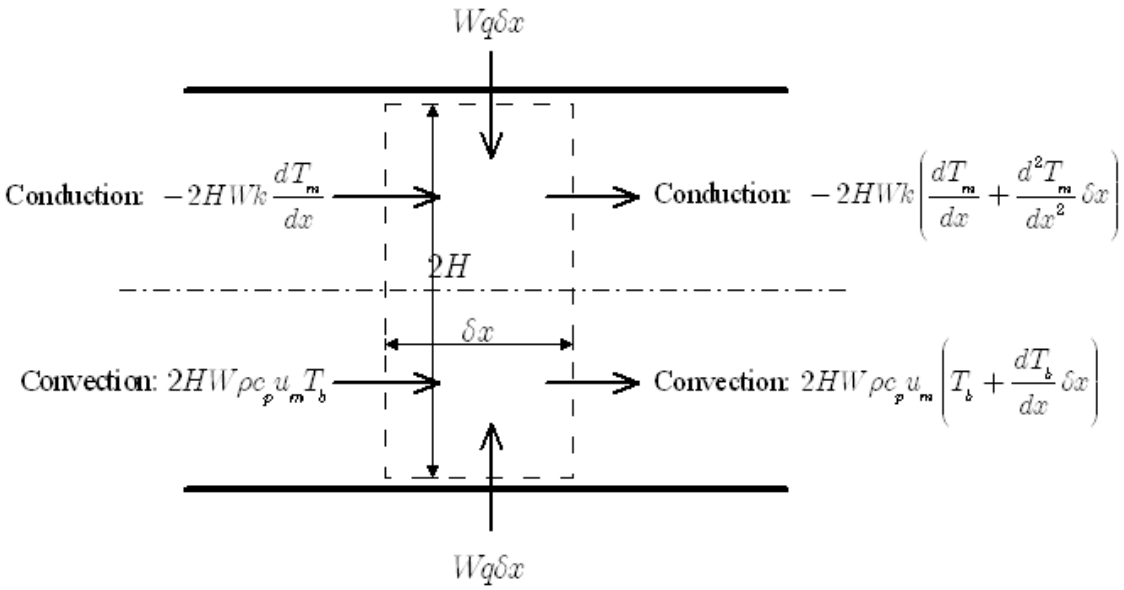

Energy conversation for a volume (W is the length in the span-wise direction)

Fig. 7

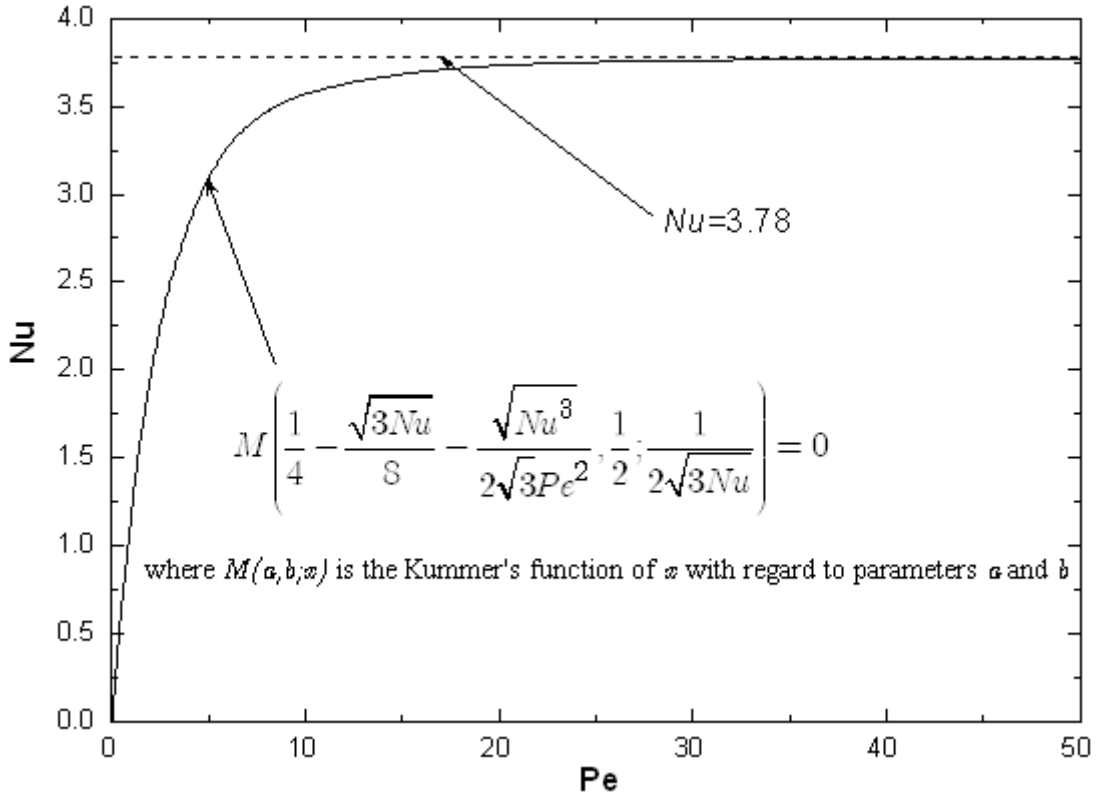

Fig. 8

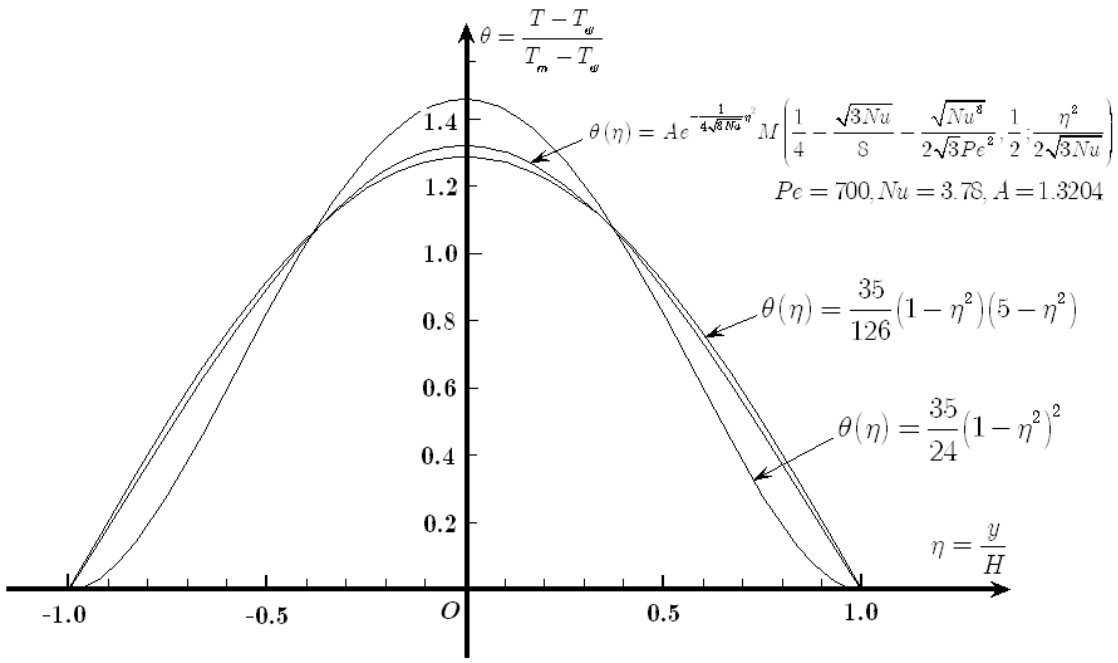
$\theta = \frac{T - T_w}{T_\infty - T_w}$
$\theta(\eta) = Ae^{-\frac{1}{4\sqrt{3}Nu}\eta^2} M\left(\frac{1}{4} - \frac{\sqrt{3Nu}}{8}, \frac{1}{2}, \frac{\eta^2}{2\sqrt{3Nu}}\right)$
$Pe = 700, Nu = 3.78, A = 1.3204$
$\theta(\eta) = \frac{35}{126}(1-\eta^2)(5-\eta^2)$
$\theta(\eta) = \frac{35}{24}(1-\eta^2)^2$
$\eta = \frac{y}{H}$
1.4
1.2
1.0
0.8
0.6
0.4
0.2
-1.0
-0.5
O
0.5
1.0

Fig. 9